Long non-coding RNA nuclear paraspeckle assembly transcript 1 regulates ionizing radiation-induced pyroptosis via microRNA-448/gasdermin E in colorectal cancer cells

FEI SU*, JUNZHAO DUAN*, JIE ZHU, HANJIANG FU, XIAOFEI ZHENG and CHANGHUI GE

Department of Experimental Hematology and Biochemistry, Beijing Key Laboratory for Radiobiology, Beijing Institute of Radiation Medicine, Beijing 100850, P.R. China

Received May 7, 2021; Accepted July 16, 2021

DOI: 10.3892/ijo.2021.5259

Abstract. Pyroptosis is mediated by gasdermins and serves a critical role in ionizing radiation (IR)-induced damage in normal tissues, but its role in cancer radiotherapy and underlying mechanisms remains unclear. Long non-coding (lnc) RNAs serve important roles in regulating the radiosensitivity of cancer cells. The present study aimed to investigate the mechanistic involvement of lncRNAs in IR-induced pyroptosis in human colorectal cancer HCT116 cells. LncRNA, microRNA (miR)-448 and gasdermin E (GSDME) levels were evaluated using reverse transcription-quantitative polymerase chain reaction. Protein expression and activation of gasdermins were measured using western blotting. The binding association between miR-448 and GSDME was assessed using the dual-luciferase reporter assay. Pyroptosis was examined using phase-contrast microscopy, flow cytometry, Cell Counting Kit-8 assay and lactate dehydrogenase release assay. IR dose-dependently induced GSDME-mediated pyroptosis in HCT116 cells. GSDME was identified as a downstream target of miR-448. LncRNA nuclear paraspeckle assembly transcript 1 (NEAT1) was upregulated in response to IR and enhanced GSDME expression by negatively regulating miR-448 expression. Notably, NEAT1 knockdown suppressed IR-induced pyroptosis, full-length GSDME expression and GSDME cleavage compared with that in irradiated cells. In addition, NEAT1 knockdown rescued the IR-induced decrease in cell viability in HCT116 cells. The findings of the present study indicated that lncRNA NEAT1 modulates IR-induced pyroptosis and viability in HCT116 cells via miR-448 by regulating the expression, but not activation of GSDME. The present study provides crucial mechanistic insight into the potential role of lncRNA NEAT1 in IR-induced pyroptosis.

Correspondence to: Professor Changhui Ge or Professor Xiaofei Zheng, Department of Experimental Hematology and Biochemistry, Beijing Key Laboratory for Radiobiology, Beijing Institute of Radiation Medicine, 27 Taiping Road, Beijing 100850, P.R. China
E-mail: chge502@163.com
E-mail: xfzheng100@126.com

*Contributed equally

Abbreviations: Casp1, caspase-1; Casp3, caspase-3; ceRNA, competing endogenous RNA; COAD, colon adenocarcinoma; DFNB59, autosomal recessive deafness type 59 protein; GAPDH, glyceraldehyde 3-phosphate dehydrogenase; GEO, Gene Expression Omnibus; GSDMD, gasdermin D; GSDME, gasdermin E; IR, ionizing radiation; LDH, lactate dehydrogenase; lncRNA, long non-coding RNA; MALAT1, metastasis-associated lung adenocarcinoma transcript 1; NEAT1, nuclear paraspeckle assembly transcript 1; NLRP1, NLR family pyrin domain containing 1; NLRP3, NLR family pyrin domain containing 3; OIP5-AS1, OIP5 antisense RNA 1; PVT1, Pvt1 oncogene; TCGA, The Cancer Genome Atlas

Key words: ionizing radiation, pyroptosis, gasdermin E, microRNA-448, nuclear paraspeckle assembly transcript 1

Introduction

Pyroptosis is a recently discovered form of lytic cell death that is characterized by cell swelling and formation of pores and large bubbles on the plasma membrane (1). Pyroptosis is predominantly stimulated by the activation of canonical caspase-1 (Casp1) and noncanonical caspase-4/5/11 (2), leading to the release of N-terminal fragments of pyroptosis execution protein, gasdermin D (GSDMD) (3). GSDMD translocates to the membrane leading to membrane perforation and subsequent infiltration of extracellular content and cell swelling (3). GSDMD is a member of the gasdermin family, which comprises gasdermin A, gasdermin B, gasdermin C, gasdermin E (GSDME) and autosomal recessive deafness type 59 protein (DFNB59) (4). The N domains of the gasdermin family with the exception of DFNB59 are capable of inducing pyroptosis (3,5). In particular, GSDME is cleaved by caspase-3 (Casp3) and switches apoptosis to pyroptosis in several cancers, which is associated with the side effects of chemotherapy and antitumor immunity (6) in breast cancer (7), lung cancer (8), gastric cancer (9) and colorectal cancer (10). Growing evidence suggests that numerous chemotherapeutic drugs, such as cisplatin and etoposide (6), may activate pyroptosis via canonical or noncanonical inflammasome pathways, including TLR and MAPK pathways (11), inhibit cancer progression

and overcome apoptosis resistance, which are major causes of cancer resistance (12).

Radiotherapy is an effective nonsurgical treatment for various solid tumors including colorectal cancer (13). Radiotherapy involves multiple pathways that regulate apoptosis, such as Bcl-2 or nuclear factor-κB pathways (14), but the regulatory mechanisms of colorectal cancer after radiation have not been fully elucidated. Pyroptosis is induced in normal tissues and cells, including the bone marrow (15), brain (16), lung (17), intestine (18) and macrophages (19), in response to radiation, as well as in tumor cells in response to chemotherapeutic drugs, such as cisplatin or 5-fluorouracil (8,9). Nevertheless, the effects of radiotherapy on pyroptosis in tumors, especially colorectal cancer and the underlying mechanisms remain unclear.

Long non-coding RNAs (lncRNAs) are non-protein coding transcriptional units that modulate various biological processes, such as gene transcription, pre-mRNA processing and splicing, transport, translation and degradation (20). LncRNAs have been implicated in breast, hepatocellular, colorectal and pancreatic cancer (21). Notably, a growing body of evidence suggests that lncRNAs serve a crucial role in the radiosensitivity of tumors and cells (22,23), especially radiation-induced DNA damage in colorectal cancer. For instance, Zhou *et al* (24) reported that WWC2 antisense RNA 1 functions as a novel competing endogenous RNA (ceRNA) that regulates fibroblast growth factor 2 expression by sponging microRNA (miR)-16 in radiation-induced intestinal fibrosis. Zou *et al* (25) reported that OIP5 antisense RNA 1 (OIP5-AS1) regulates radioresistance in colorectal cancer cells by targeting dual specificity YAK1-related kinase via miR-369-3p.

Several reports have demonstrated that lncRNAs regulate the mediators of pyroptosis, including NLR family pyrin domain containing 1 (NLRP1) (26), NLR family pyrin domain containing 3 (NLRP3) (27), Casp1 (28) and Casp3 (29). Nevertheless, the non-coding RNAs that regulate GSDMs, the key execution proteins of pyroptosis have not been identified.

Hence, the present study aimed to investigate the regulatory roles of lncRNAs implicated in ionizing radiation (IR)-induced pyroptosis in colorectal cancer cells by targeting the GSDME. The present study provides novel insights into the molecular mechanisms underlying IR-induced damage in cancer radiotherapy and may lay a theoretical foundation for further therapeutic development in colorectal cancer.

Materials and methods

Cell culture and radiation treatment. 293T cells and human colorectal cancer HCT116 cells (American Type Culture Collection) were cultured in Dulbecco's modified Eagle's medium (Gibco; Thermo Fisher Scientific Inc.) containing 10% fetal bovine serum (PAN-Biotech GmbH.), 100 U/ml penicillin and 100 μg/ml streptomycin at 37˚C. The cells were irradiated with 0, 8, 12 and 16 Gy at 25˚C with a dose rate of 87 cGy/min using a ^{60}Co g-ray source at Beijing Institute of Radiation Medicine (Beijing, China).

miRNA prediction. The potential regulatory miRNAs that bind to the 3'-untranslated region (3'-UTR) of GSDME were screened for using the miRDB (http://mirdb.org/), miRWalk (http://mirwalk.umm.uni-heidelberg.de/), microRNA.org (http://www.microrna.org/) and TargetScan databases (http://www.targetscan.org/).

Plasmids, miRNA mimics and small interfering (si)RNAs. miRNA expression plasmids were generated by cloning pre-miRNA and flank sequences into pcDNA3.0 (Invitrogen; Thermo Fisher Scientific Inc.) as described previously (30) and used in luciferase reporter assays and reverse transcription-quantitative PCR (RT-qPCR) experiments. miR-375, miR-379, and miR-448 mimics were obtained from Shanghai GenePharma Co., Ltd. GSDME was silenced using a siRNA targeting human GSDME (siGSDME) (31). Nuclear paraspeckle assembly transcript 1 (NEAT1) was silenced using siRNA targeting human NEAT1 isoform-1 (siNEAT1-1), isoform-2 (siNEAT1-2) or both isoforms (siNEAT1-1+2) (32). The pre-miRNA cloning, PCR primer, miRNA mimics and siRNA sequences are listed in Table SI. The scrambled negative control RNAs for miRNA mimics and siRNA were obtained from Shanghai GenePharma Co., Ltd. The control vector pcDNA3.0 was used for luciferase reporter assays and RT-qPCR analysis of miRNAs.

Transfection. 293T or HCT116 cells were seeded at a density of 3-5x10^5 cells/well in 6-well plates and cultured to 50% confluence at 37˚C. Cells were then transfected with miRNA mimics or siRNAs at 100 pmol/well using Lipofectamine 2000® reagent (Invitrogen; Thermo Fisher Scientific Inc.) according to the manufacturer's instructions. The RT-PCR and western blotting experiments were performed at 48 h post-transfection, or the HCT116 cells were irradiated at 12 h post-transfection followed by subsequent experiments as indicated.

Luciferase reporter assays. The GSDME 3'-UTR reporter plasmid was generated by inserting the 3'-UTR fragment of human GSDME into pGL3-basic vector (Promega Corporation) using *Xba*I/*Nde*I. The GSDME 3'-UTR reporter plasmids with a mutation in either one or both of the two miR-448-binding sites were generated using the QuickMutation kit (Beyotime Institute of Biotechnology). 293T cells were seeded at a density of 1x10^5 cells/well in 24-well plates. The next day, cells were transfected with 100 ng luciferase reporter plasmid, 1 ng *Renilla* luciferase expression plasmid (pRL-TK; Promega Corporation) and 400 ng miR-370, -375, -376, -379, -448, -452 expression plasmid or control vector pcDNA3.0 plasmid using Lipofectamine 2000® reagent (Invitrogen; Thermo Fisher Scientific Inc.) according to the manufacturer's instructions. After 48 h, the cells were lysed and assessed following the Dual-Luciferase Reporter Assay System (Promega Corporation) protocol. Luminescence measurements were obtained using an FB12 luminometer (Berthold Detection Systems GmbH). Relative luciferase activities were calculated by normalizing the ratio of firefly/*Renilla* luciferase to that of control cells.

Cell viability assay. HCT116 cells were seeded at a density of 5x10^3 cells/well in a 96-multiwell plate and irradiated or transfected with GSDME siRNA, NEAT1 siRNAs or miR-448 mimics. HCT116 cells were cultured for 72 h and subsequently

analyzed using the Cell Counting Kit-8 assay (Dojindo Molecular Technologies, Inc.) according to the manufacturer's instructions. Briefly, 100 μl mixture (CCK-8 reagent:medium, 1:10) was added into each well and the cells were incubated at 37˚C for 1.5 h, then absorbance at 450 nm was measured using a microplate reader (LabSystems Multiskan MS; Thermo Fisher Scientific Inc.).

Pyroptotic cell observation. HCT116 cells were irradiated at 0, 8, 12 and 16 Gy, and subsequently cultured for 48 h. Pyroptotic cells were observed under a phase-contrast microscope (Nikon Corporation) and five fields per group were assessed.

Lactate dehydrogenase (LDH) release assay. LDH released from cultured HCT116 cells into media was measured using the CytoTox 96 Non-Radioactive Cytotoxicity Assay (Promega Corporation) according to the manufacturer's instructions. LDH release was calculated as % LDH release=(sample LDH activity-background LDH)/(total LDH activity-background LDH) x100%.

Flow cytometry. HCT116 cells were irradiated for 24 h, harvested, dissociated into single cell suspensions with 0.25% trypsin at 37˚C for 5 min and stained with APC-conjugated Annexin V and 7-aminoactinomycin D (7-AAD) using the Annexin V-APC staining kit (cat. no. 62700-80; BioGems International, Inc.) according to the manufacturer's instruction. Cells were analyzed by flow cytometry using a FACSCalibur (BD Biosciences). Data were further analyzed using FlowJo v10.0 (FlowJo, LLC).

RT-qPCR. Total RNA was extracted from cultured HCT116 cells using TRIzol® (Invitrogen; Thermo Fisher Scientific Inc.). cDNA was reverse transcribed using the ImProm-II Reverse Transcription System (Promega Corporation) according to the manufacturer's instructions. Quantitative polymerase chain reaction (PCR) amplification was performed using the SYBR green method (Takara Bio, Inc.) using the Bio-Rad IQTM5 Multicolor Real-time PCR Detection System (Bio-Rad Laboratories, Inc.). PCR primer sequences were obtained from OriGene Technologies Inc. or designed using NCBI Primer-BLAST (https://www.ncbi.nlm.nih.gov/tools/primer-blast/). Primer sequences were listed in Table SI. The reaction conditions were as follows: 95˚C for 1 min, then 40 cycles of 10 sec at 95˚C, 30 sec at 55˚C and 30 sec at 72˚C. The threshold cycle (Ct) values of miRNAs were normalized to those of U6, and those of the remaining genes were normalized to glyceraldehyde 3-phosphate dehydrogenase (GAPDH). Differential expression was calculated according to the $2^{-\Delta\Delta Cq}$ method (33).

Western blotting. Proteins were extracted from HCT116 cells using the radioimmunoprecipitation assay buffer with proteinase inhibitors (Thermo Fisher Scientific, Inc.) Protein concentration was determined using the bicinchoninic acid method. Subsequently, ~30 μg protein was separated by SDS-PAGE on 12% gels and transferred to a polyvinylidene fluoride membrane. The membrane was blocked with 8% nonfat milk in TBS-0.1% Tween-20 at 25˚C for 2 h and then incubated with anti-GSDMD (1:2,000; cat. no. ab210070; Abcam), anti-GSDME (1:2,000; cat. no. ab215191; Abcam) or the loading control anti-GAPDH (1:2,000; cat. no. AC001; ABclonal Biotech Co., Ltd.) antibodies at 4˚C overnight. After washing, the HRP-conjugated secondary antibodies (1:5,000; cat. no. SA00001-2; ProteinTech Group, Inc.) were incubated at 25˚C for 2 h. The protein bands were visualized using an enhanced chemiluminescent kit (MilliporeSigma). Experiments were performed at least in duplicate and similar results were obtained.

Immunohistochemistry. Immunostaining images of GSDME in normal colon and colon adenocarcinoma tissues were obtained from the Human Protein Atlas (http://www.proteinatlas.org). The examples of the pictures were selected from the normal (male, patient id: 1857; female patient id: 1423) and colon adenocarcinoma (male, patient id: 3408; female patient id: 1958) tissues, which were stained with antibody CAB019306. The images are available at v.20.1.proteinatlas.org.

Gene expression omnibus (GEO) and the cancer genome atlas (TCGA) data analyses. LncRNA NEAT1 and miR-448 expression data were obtained from PubMed GEO (https://www.ncbi.nlm.nih.gov/geo/) (GSE65292, GSE8704, GSE43310, GSE137013) and NCBI Sequence Read Archive (SRA, http://www.ncbi.nlm.nih.gov/Traces/sra) (PRJNA644335) databases or from supplementary data from Rogers *et al* (34). Expression and overall survival analyses for NEAT1 and GSDME in colon adenocarcinoma (COAD) from TCGA database (http://gepia.cancer-pku.cn) were performed using the Gene Expression Profiling Interactive Analysis online tool (http://gepia.cancer-pku.cn/) (35). The threshold for defining high/low gene expression levels was set using the following criteria: 50% of the patients were categorized into the high-expression group and the remaining 50% into the low-expression group.

Statistical analyses. Student's unpaired two-tailed t-test or one-way analysis of variance followed by Tukey's post hoc test was used to assess experimental data using GraphPad Prism 8 software (GraphPad Software, Inc.). The Kaplan-Meier analysis and log-rank test was used for overall survival analysis. The data are presented as means ± standard error of the mean from three biological replicates. $P<0.05$ was considered to indicate a statistically significant difference.

Results

IR-induced GSDME-mediated pyroptosis in HCT116 cells. To elucidate the mechanisms underpinning IR-induced damage in colonic epithelium, the effects of IR on human colorectal carcinoma HCT116 cells were investigated at 0, 8, 12 and 16 Gy. Cell viability analysis revealed that IR dose-dependently inhibited cell growth by ~50% at 72 h post-irradiation ($P<0.01$) (Fig. 1A). Flow cytometry analysis revealed that IR dose-dependently increased the percentage of dead cells (double positive for 7-AAD and Annexin V, which provides an approximate quantitative estimate of pyroptotic cells) (36) at 48 h post-irradiation ($P<0.05$) (Fig. 1B). Pyroptotic cells were observed using a phase-contrast microscope; a lower number of dilated cells was observed under 12 Gy and a higher number

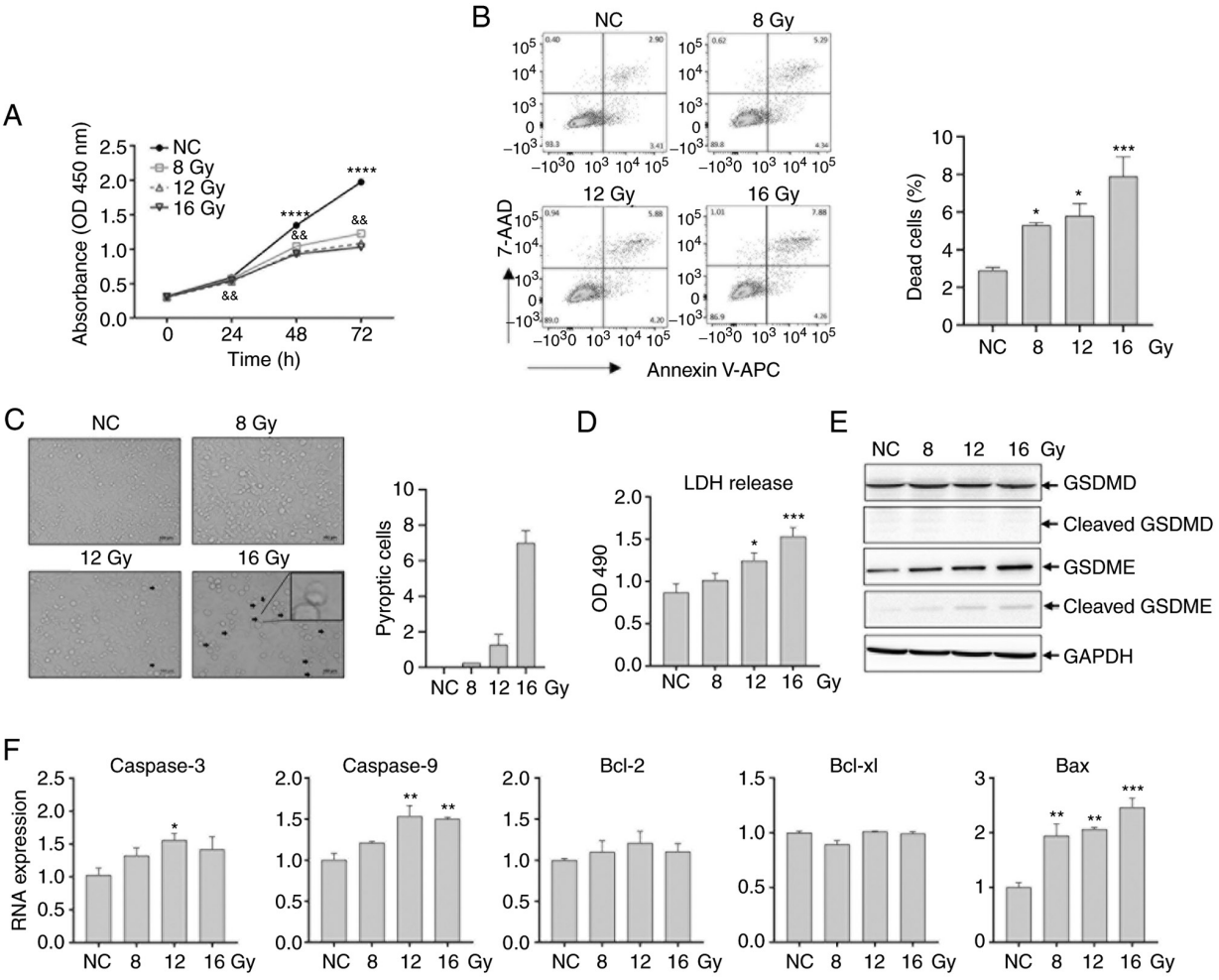

Figure 1. Irradiation-induced pyroptosis in colorectal cancer HCT116 cells. HCT116 cells were irradiated with 8.0, 12.0 and 16.0 Gy. (A) Cell viability was analyzed using a Cell Counting Kit-8 assay at 72 h post-irradiation. ****P<0.0001 for normal control vs. 8.0 Gy; $^{\&\&}$P<0.01 for 8.0 Gy vs. 12.0 Gy. (B) Flow cytometry analysis of irradiated HCT116 cells at 48 h. (C) Pyroptotic cells with large bubbles were observed at 48 h. The arrows indicate pyroptotic cells. The number of pyroptotic cells per field is indicated. (D) LDH released in media was measured at 24 h. (E) Total protein was extracted at 24 h. The expression and activation of GSDMD and GSDME were analyzed using western blotting. Glyceraldehyde 3-phosphate dehydrogenase was used as a loading control. (F) *Caspase-3, -9, Bcl-2, Bcl-xl and Bax* expression were analyzed using RT-qPCR in HCT116 cells at 48 h. GAPDH was used as the control. *P<0.05, **P<0.01, ***P<0.001, ****P<0.0001. OD, optical density; RT-q, reverse transcription-quantitative; GSDMD, gasdermin D; GSDME, gasdermin E; LDH, lactate dehydrogenase; NC, negative control, comprising nonirradiated cells.

under 16 Gy compared with those in the control group, which showed that pyroptotic cell percentage may increase with dose (Fig. 1C). LDH released into media from irradiated HCT116 cells exhibited a significant gradual increase in response to dose of irradiation (P<0.05) (Fig. 1D). Western blotting analysis revealed that full-length and cleaved GSDMD expression remained unchanged with increasing radiation dose (Fig. 1E). In contrast, full-length GSDME protein expression was upregulated and cleaved GSDME protein expression increased continuously with increasing radiation dose (Fig. 1E).

It has previously been reported that radiation may induce apoptosis by selectively active caspase-9 and caspase-3/7 and both proapoptotic and antiapoptotic Bcl-2 family proteins (37). The expression of apoptosis-related genes in HCT116 cells was assessed after irradiation. The results demonstrated that the expression levels of Caspase-3 and Caspase-9 were significantly increased at -12 Gy (P<0.05), and those of the proapoptotic gene Bax were significantly increased at all doses (P<0.01), but that of antiapoptotic genes Bcl-2 and Bcl-xl was unchanged (Fig. 1F). These results indicated IR may induce caspases- and Bax-mediated apoptosis and GSDME-mediated pyroptosis in HCT116 cells.

GSDME is a target of miR-448. Next, the upstream factors of GSDME in human colorectal carcinoma cells were investigated based on the literature suggesting that miRNAs regulate cellular function by binding to the 3'-UTR of target genes (38). In this regard, 4 databases (including miRDB, miRWalk, microRNA.org and TargetScan) were screened and 6 candidates (miR-370, miR-375, miR-376, miR-379, miR-448 and miR-452) were obtained (Fig. 2A). 293T cells were then transfected with these miRNA plasmids and these miRNAs were highly expressed compared with cells transfected with control plasmid pcDNA3.0 (Fig. 2B). Transcriptional activity of GSDME was analyzed using GSDME 3'-UTR luciferase reporter assays, and miR-375, miR-379 and miR-448 were revealed as potentially targeting GSDME, but miR-370, miR-376 and miR-452 were excluded because their luciferase activities remained unchanged (Fig. 2C). The role of potential miRNAs were assessed by analyzing the expression of

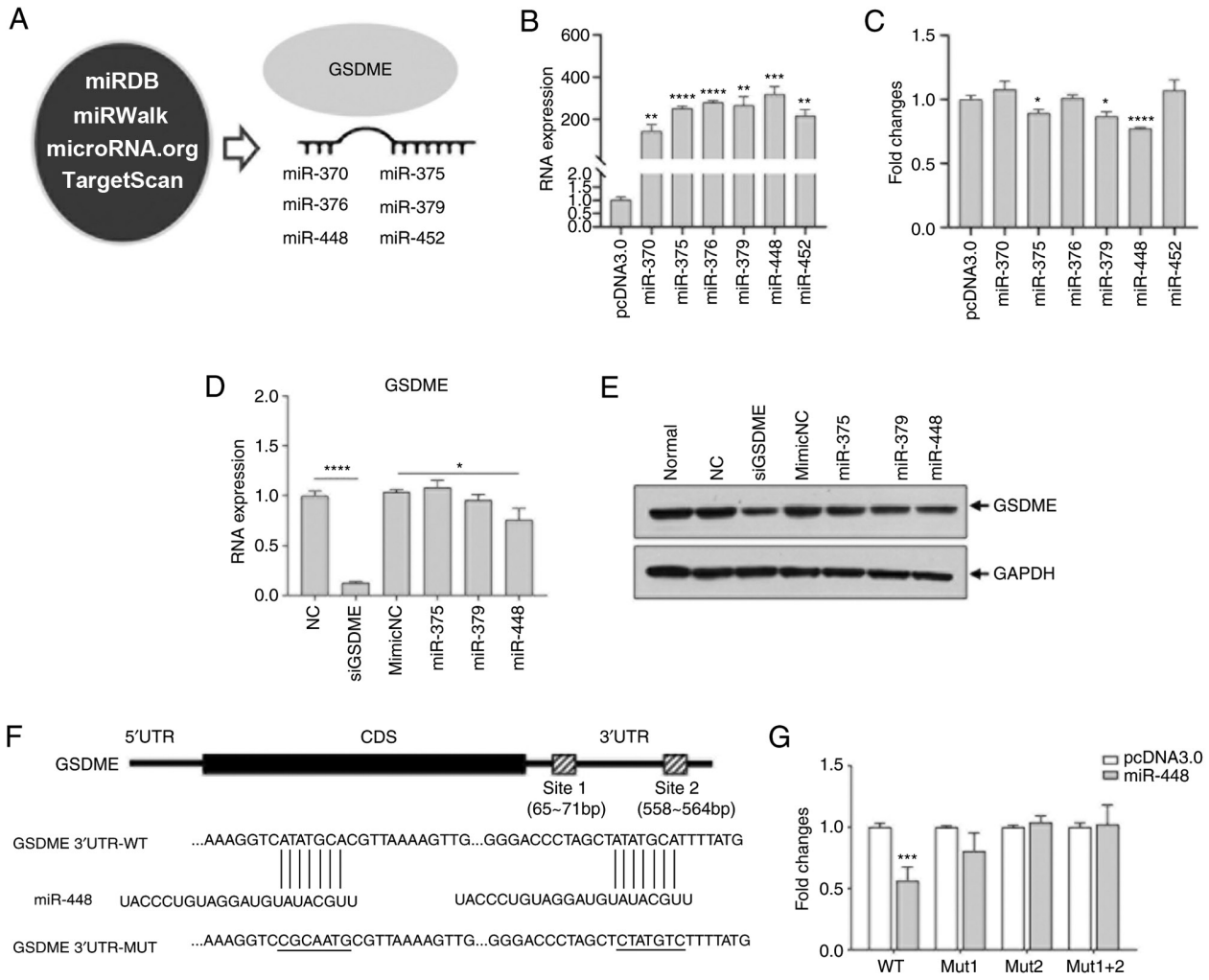

Figure 2. GSDME is a target of miR-448. (A) miRNAs identified by screening of miRDB, miRWalk, microRNA.org and TargetScan databases. (B) 293T cells were transfected with GSDME 3'-UTR luciferase reporter plasmid and miRNA vectors, the expression of each miRNA was verified by RT-qPCR. (C) Luciferase activity was measured using a dual-luciferase reporter assay. (D) Selection of potential regulatory miRNAs (miR-375-3p, miR-379-3p and miR-448) was verified with RT-qPCR. GSDME siRNA was used as a positive control. (E) 293T cells were transfected with GSDME siRNA and selected miRNA mimetics. GSDME expression was analyzed using western blotting. (F) Potential binding sites between miR-448 and GSDME were predicted by miRBase. (G) Either or both of 2 miR-448 binding sites in GSDME 3'-UTR reporter plasmids were mutated followed by transfection into 293T cells. A luciferase activity assay was subsequently performed. *P<0.05, **P<0.01, ***P<0.001, ****P<0.0001, compared with the pcDNA3.0 group unless otherwise indicated. RT-q, reverse transcription-quantitative; GSDME, gasdermin E; miR, microRNA; si, small interfering; NC, negative control; MUT, mutant; WT, wildtype; UTR, untranslated region; normal, untransfected cells.

GSDME using RT-qPCR and western blotting, which revealed that miR-448 mimic significantly inhibited the expression of GSDME at the mRNA and protein levels compared with those in cells transfected with the mimic control miRNA (P<0.05), and siGSDME also decreased GSDME expression (P<0.0001) (Fig. 2D and E). As GSDME contained 2 miR-448 binding sites in its 3'-UTR sequences, mutant GSDME 3'-UTR luciferase reporter plasmids with mutations in either or both binding sites were generated (Fig. 2F). Mutations of either or both miR-448 binding sites rescued decreased luciferase activity to control levels (Fig. 2G), suggesting that GSDME was a downstream target of miR-448.

Identification of lncRNAs targeting miR-448/GSDME in HCT116 cells. To examine the hypothesis regarding ceRNA and the association between miR-448 and GSDME, the potential upstream lncRNAs of miR-448 were investigated. Several lncRNAs have been reported to act as ceRNAs that regulate miR-448, including metastasis-associated lung adenocarcinoma transcript 1 (MALAT1), NEAT1, OIP5-AS1, Pvt1 oncogene (PVT1) and small nucleolar RNA host gene 1 (SNHG1) (Table I) (39-43). The expression of these lncRNAs was investigated in HCT116 cells according to radiation dose and over time. Given that IR dose-dependently increased pyroptosis, it was hypothesized that the expression of these lncRNAs would be significantly upregulated if they were involved in the regulation of GSDME expression via miR-448.

The expression of MALAT1 exhibited a trend to be upregulated with radiation dose, but this did not reach significance (Fig. 3A). OIP5-AS1 expression was downregulated with IR dose, whereas the expression of PVT1 and SHNG1 was not regulated in response to IR dose (Fig. 3A). Notably, NEAT1 expression was significantly upregulated with an increase in IR dose (P<0.01) (Fig. 3A). IR time-dependently increased NEAT1 expression (P<0.001), whereas no significant temporal effects of IR on other lncRNAs were observed (Fig. 3B).

Table I. List of miR-448 related ceRNAs.

Author, year	lncRNA	Full name (Aliases)	miRNA	Target	Tissue	Function	(Refs.)
Bamodu *et al* 2016	MALAT1	Metastasis Associated Lung Adenocarcinoma Transcript 1	miR-448	KDM5B	Breast cancer	Promotes aggressive breast cancer	(39)
Jiang *et al* 2018	NEAT1	Nuclear Paraspeckle Assembly Transcript 1	miR-448	ZEB1	Breast cancer	Contribute progression	(40)
Deng *et al* 2018	OIP5-AS1	OIP5 Antisense RNA 1	miR-448	Bcl-2	Lung adenocarcinoma	As oncogene	(41)
Zhao *et al* 2018	PVT1	Pvt1 Oncogene	miR-448	/	Pancreatic cancer	Promotes proliferation and migration	(42)
Pei *et al* 2018	SNHG1	Small Nucleolar RNA Host Gene 1	miR-448	IDO	Breast cancer	Immune escape of breast cancer	(43)

ceRNA, competing endogenous RNA; miRNA, microRNA; ZEB1, zinc finger E-box binding homeobox 1; IDO, indoleamine 2,3-dioxygenase; KDM5B, lysine demethylase 5B.

NEAT1 expression in microarray or sequencing data from the PubMed GSE or SRA database and the literature and identified that NEAT1 expression was increased in human blood (44), monkey thymus (45), mouse embryonic fibroblast cells (46), mouse bone marrow (47) and mouse spleen (48) after irradiation (Fig. 3C-H), suggesting that NEAT1 expression was ubiquitously upregulated in response to IR.

NEAT1 regulates GSDME expression. To confirm the functional association between NEAT1 and GSDME, first, the expression of GSDME protein was found to be higher in normal colon compared with COAD tissue in The Human Protein Atlas database (Fig. 4A). Next, NEAT1 and GSDME expression and the overall survival rate in COAD was assessed using TCGA data, which revealed a positive association between NEAT1 and GSDME levels and the advanced stages of COAD (Fig. 4B). Patients with COAD with higher NEAT1 and GSDME expression had lower overall survival, suggesting that they are positively associated in COAD (Fig. 4C). Secondly, NEAT1 was knocked down in HCT116 cells by transfecting cells with siRNAs against isoform NEAT1-1, NEAT1-2 or combined isoforms NEAT1-1+2. Treatment with siNEAT1-1, siNEAT1-2 and siNEAT1-1+2 significantly decreased NEAT1 expression compared with treatment with the negative control ($P<0.05$) (Fig. 4D), which indicated that siRNAs against NEAT1 were effective. However, GSDME expression was not affected by siNEAT1-1 or siNEAT1-2 treatment, but was downregulated following transfection of cells with siNEAT1-1+2 ($P<0.01$) (Fig. 4E). miR-448 expression was also confirmed to be upregulated in HCT116 cells transfected with siNEAT1-1+2 compared with those transfected with negative control siRNA ($P<0.01$) (Fig. 4F). Western blots revealed that full-length GSDME protein expression was downregulated following treatment with siNEAT1-1+2, but remained unchanged following treatment with siNEAT1-1 and siNEAT1-2 compared with normal control levels (Fig. 4G). In addition, the activated form of the N-terminal fragment of cleaved GSDME was not detected (Fig. 4G). This downregulation could be rescued by co-transfection of miR-448 mimetic with siNEAT1-1+2 in HCT116 cells ($P<0.01$) (Fig. 4H), supporting the involvement of miR-448 in the regulation of GSDME by NEAT1.

NEAT1 promotes radioresistance by enhancing pyroptosis via miR-448/GSDME. To further investigate the regulation of lncRNAs/miR-448/GSDME in IR-induced pyroptosis in HCT116 cells, HCT116 cells were irradiated with increasing doses. A gradual decrease in expression of miR-448 was observed ($P<0.001$; Fig. 5A), which was negatively associated with the expression of NEAT1 and GSDME in irradiated HCT116 cells (Figs. 3A and 5B). Based on the PubMed GEO database (34,47), the expression of miR-448 was downregulated in the mouse lung, but not in the heart or bone marrow suggesting that miR-448 may be regulated in a tissue-specific manner in response to IR (Fig. 5C and D). Similarly, TCGA data analysis demonstrated that GSDME exhibited a tissue-specific differential expression between tumors and normal tissues (Fig. S1). To confirm the regulation of NEAT1 and miR-448 in IR-induced pyroptosis, HCT116 cells were transfected

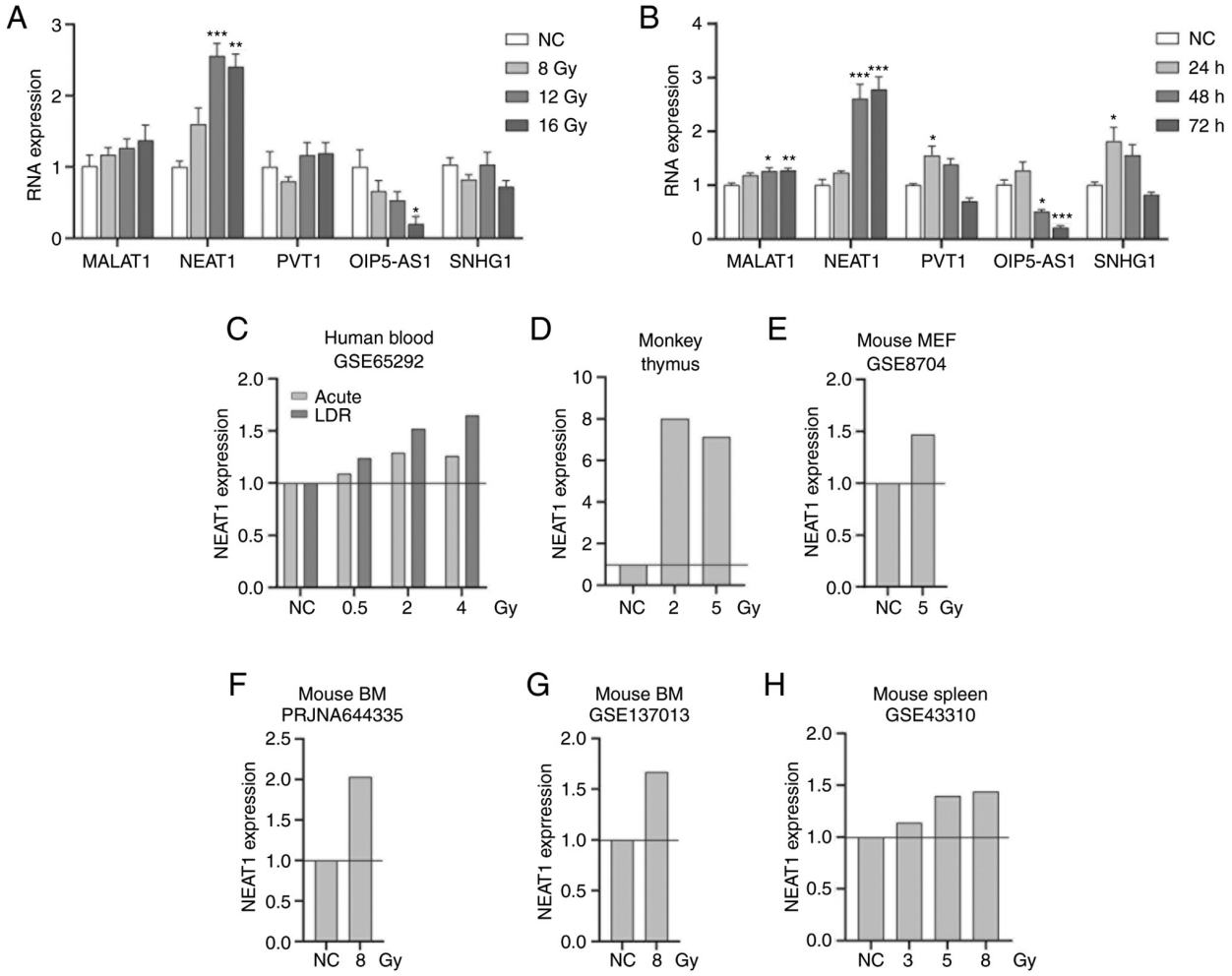

Figure 3. Induction of miR-448 ceRNAs in HCT116 cells by radiation. (A) HCT116 cells were irradiated with 8.0, 12.0 and 16.0 Gy. The expression of MALAT1, nuclear NEAT1, OIP5-AS1, PVT1 and SHNG1 was analyzed at 48 h post-irradiation using RT-qPCR. (B) HCT116 cells were irradiated with 12.0 Gy. The expression of lncRNAs MALAT1, NEAT1, OIP5-AS1, PVT1 and SHNG1 was analyzed at 24, 48 and 72 h using RT-qPCR. (C-H) NEAT1 expression in human blood, monkey thymus, mouse embryonic fibroblast cells, mouse bone marrow and mouse spleen based on the PubMed GEO (GSE65292, GSE8704, GSE43310, GSE137013) and PubMed Sequence Read Archive database (PRJNA644335) or supplementary data from Rogers *et al* (34). *P<0.05, **P<0.01, ***P<0.001, compared with the NC group. lncRNA, long non-coding RNA; MEF, mouse embryonic fibroblast; GEO, Gene Expression Omnibus; RT-q, reverse transcription-quantitative; BM, bone marrow; MALAT1, metastasis-associated lung adenocarcinoma transcript 1; NEAT1, nuclear paraspeckle assembly transcript 1; OIP5-AS1, OIP5 antisense RNA 1; PVT1, Pvt1 oncogene; SNHG1, small nucleolar RNA Host Gene 1; ceRNA, competing endogenous RNA; NC, negative control, comprising nonirradiated cells or as defined in databases.

with siNEAT1-1+2 and miR-448 mimetics before irradiation. Knockdown of NEAT1 increased miR-448 expression (P<0.01) and resulted in a decrease in LDH release and rescued cell viability in radiated HCT116 cells compared with irradiated cells transfected with negative control RNA (P<0.05) (Fig. 5E-G); similar results were obtained from overexpression of miR-448, suggesting a regulatory role of NEAT1/miR-448 on viability of human colorectal cancer cells via pyroptosis (P<0.05) (Fig. 5F-G). The expression of GSDME mRNA and full-length protein was downregulated, in accordance with the changes in morphology and LDH release following transfection with siNEAT1 and miR-448 mimetics. Expression of the cleaved N-terminal fragment of GSDME was also decreased and the ratios of GSDME-N vs. GSDME-F were not significantly different (Fig. 5H-I). Taken together, lncRNA NEAT1 might sponge miR-448 and promote radioresistance by enhancing IR-induced pyroptosis in human colorectal cancer HCT116 cells via regulating the expression, but not activation, of GSDME.

Discussion

The present study demonstrated that in addition to enhancing apoptosis via caspases and the bcl-2 family, IR dose-dependently induced pyroptosis in human colorectal cells and identified GSDME as a target of miR-448. In the present study, miR-448 activity was rescued by mutations in either or both of the 2 miR-448 binding sites in GSDME 3'-UTR. In addition, the present study demonstrated that miR-448 inhibited GSDME-mediated pyroptosis and highlighted that the lncRNA NEAT1 as a potential upstream driver of miR-448. Notably, the present study observed that lncRNA NEAT1 knockdown regulated radiosensitivity through IR-induced pyroptosis and viability by regulating the expression, but not activation of full-length GSDME. Collectively, the findings of the present study indicated the dose-dependent effects of IR on pyroptosis in human colorectal carcinoma HCT116 cells via GSDME activation and underscored the critical role of lncRNA NEAT1 in

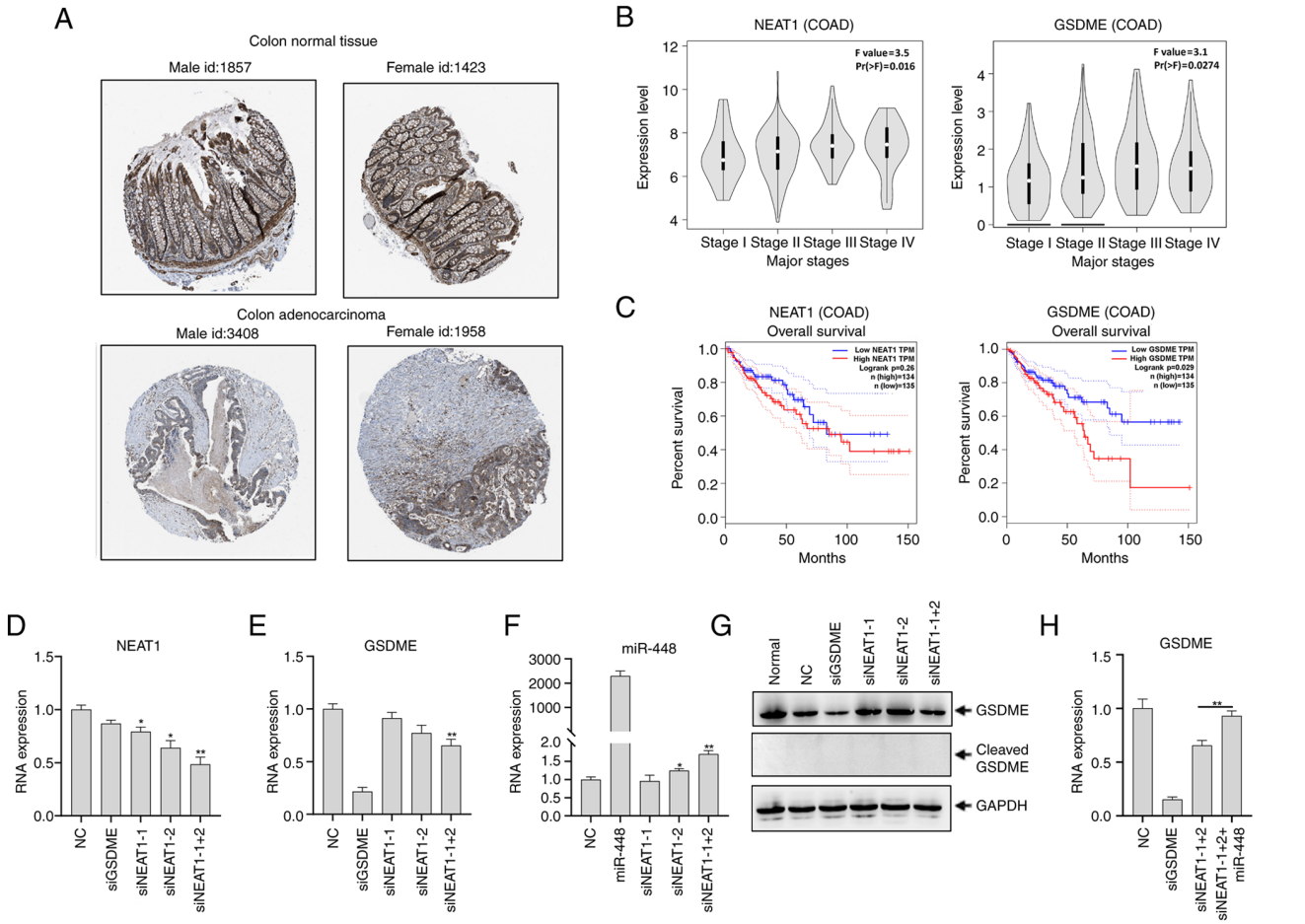

Figure 4. lncRNA NEAT1 upregulates GSDME via miR-448. (A) GSDME expression in human COAD was obtained from Human Protein Atlas (http://www.proteinatlas.org). The examples of the pictures by sex and patient id are shown and the images are available at v.20.1 www.proteinatlas.org. (B) Expression of lncRNA NEAT1 and GSDME in the major stages of COAD. (C) Overall survival analysis of NEAT1 and GSDME in COAD from the Cancer Genome Atlas database using the Gene Expression Profiling Interactive Analysis online tool. (D-G) HCT116 cells were transfected with siGSDME, siNEAT1-1, siNEAT1-2, siNEAT1-1+2, or negative control siRNA. After 48 h, (D) NEAT1 expression and (E) *GSDME* expression were analyzed using RT-qPCR. GAPDH was used as a control. (F) miR-448 expression was analyzed using RT-qPCR in HCT116 cells after transfection with siNEAT1-1, siNEAT1-2 and siNEAT1-1+2. (G) Expression of full-length and cleaved GSDME was analyzed using western blotting. GAPDH was used as a loading control. (H) *GSDME* mRNA expression was analyzed using RT-qPCR in HCT116 cells after transfection with siGSDME, siNEAT1-1+2, or co-transfection with siNEAT1-1+2 and miR-448 mimetics. *P<0.05, **P<0.01 compared with the NC group unless otherwise indicated. RT-q, reverse transcription-quantitative; GSDME, gasdermin E; miR, microRNA; si, small interfering; NEAT1, nuclear paraspeckle assembly transcript 1; lncRNA, long non-coding RNA; COAD, colon adenocarcinoma; HR, hazard ratio; NC, negative control (comprising cells transfected with NC siRNA); normal, untransfected cells.

IR-induced pyroptosis via the regulation of miR-448 and expression, but not cleavage of GSDME.

Previous studies have reported that pyroptosis is induced in the normal intestine or colon via activation of Casp1/GSDMD in ulcerative colitis injury (49-51) or in response to IR (18,52). A study demonstrated that pyroptosis in human colorectal cancer cells is induced by chemotherapeutic drugs, such as lobaplatin via Casp3/GSDME activation rather than Casp1/GSDMD (10). However, GSDMD has also been implicated in regulation of pyroptosis in colon cancer (53). In this regard, low expression of GSDMD was associated with poor colorectal cancer prognosis and lipopolysaccharide induced GSDMD-mediated pyroptosis. Additionally, overexpression of GSDMD in HT29 cells reduced cell survival and induced cell death (48). Hence, both GSDMD and GSDME are thought to regulate pyroptosis in colorectal cancer cells depending on pathological state or type of stimuli (10,53). The findings of the present study indicated that GSDME, but not GSDMD, induced pyroptosis in human colorectal cancer HCT116 cells in response to IR, which resembles the regulatory mechanism of pyroptosis in chemotherapy (6). This finding of the present study provides a novel mechanism of IR-induced damage, in addition to apoptosis and necrosis in cancer radiotherapy.

ceRNAs serve crucial roles in multiple physiological and pathological processes (24,40,54). ceRNAs have been reported to regulate pyroptosis regulators. For instance, HOX transcript antisense RNA/miR-455-3p regulated NLRP1-mediated inflammasome activation and X inactive specific transcript/miR-133-3p or maternally expressed 3/miR-7a-5p regulated NLRP3-mediated inflammasome activation (55,56). In the present study, pyroptosis execution protein GSDME was first identified as a target of miR-448 and secondly, it was identified that ceRNA NEAT1/miR-448 may regulate IR-induced GSDME-mediated pyroptosis and viability in human colorectal cancer cells. Other lncRNAs may also sponge miR-448, but they were not upregulated by IR, suggesting the absence of regulatory effects on miR-448 and IR-induced pyroptosis in the present study. Notably, expression

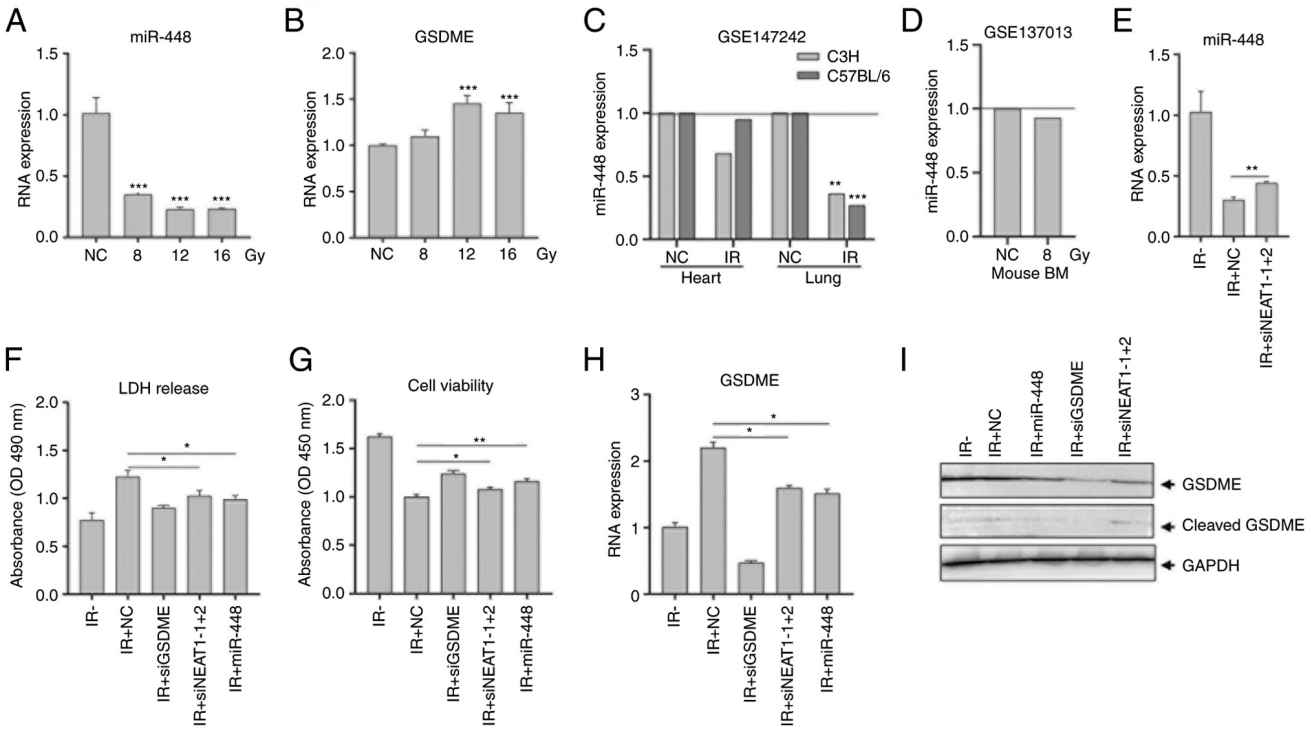

Figure 5. NEAT1 promotes radioresistance by enhancing pyroptosis via modulating miR-448/GSDME. (A and B) HCT116 cells were irradiated with 8.0, 12.0 and 16.0 Gy. Expression of miR-448 and GSDME were analyzed using RT-qPCR. (C and D) miR-448 expression in the mouse heart and lung after irradiation from the Gene Expression Omnibus dataset GSE147242 and in mouse bone marrow from GSE137013. (E-I) HCT116 cells were transfected with siNEAT1-1+2, miR-448 mimetics or negative control siRNA and then irradiated with 12.0 Gy at 12 h post-transfection. (E) Expression of miR-448 was analyzed using RT-qPCR at 48 h post-irradiation. (F) LDH released in media was measured at 24 h. (G) Cell viability was analyzed using a Cell Counting Kit-8 assay at 72 h. (H) Expression of *GSDME* was analyzed using RT-qPCR at 48 h. (I) Expression and activation of GSDME protein were analyzed at 48 h using western blotting. GAPDH was used as a loading control. *P<0.05, **P<0.01, ***P<0.001 compared with the NC group unless otherwise indicated. RT-q, reverse transcription-quantitative; IR, ionizing radiation; LDH, lactate dehydrogenase; BM, bone marrow; GSDME, gasdermin E; miR, microRNA; si, small interfering; NEAT1, nuclear paraspeckle assembly transcript 1; miR, microRNA; NC, negative control [comprising nonirradiated cells or animals in (A-D) or cells transfected with NC siRNA in (F-I)].

data in the present study demonstrated that IR-triggered miR-448 downregulation, but not NEAT1 upregulation, which may be tissue-specific, with consideration of tissue-specific differential expression of GSDME in tumors. The results of the present study indicated a complex regulation of GSDME by NEAT1/miR-448 in cancer radiotherapy.

Previous studies have shown that NEAT1 knockdown repressed proliferation, induced apoptosis (57,58), or promoted the fluorouracil sensitivity in colorectal cancer cells (59,60), but inhibited radioresistance by inducing G_0/G_1 arrest and apoptosis in cervical cancer (61) or enhanced radioresistance by depressing apoptosis in nasopharyngeal carcinoma (62). The findings of the present study suggested that NEAT1 knockdown was involved in suppression of IR-induced pyroptosis, which may contribute to enhancing radioresistance and a provided new approach for understanding the mechanism of NEAT1 in cancer therapy. NEAT1 is induced by genotoxic stress such as DNA damage and is upregulated by p53 (63), which may act as a transcriptional regulator of multiple genes, including puma and p21, that are associated with cell survival and cancer progression (64,65). Hence, IR might regulate NEAT1 via p53-mediated pathways and subsequently affect pyroptosis and viability in human colorectal cancer cells via the miR-448/GSDME axis.

GSDME cleavage is key for cell membrane rupture and pyroptosis (11). The results of the present study, demonstrated that GSDME cleavage and full-length GSDME expression were inhibited by siNEAT1 or miR-448 overexpression. The level of GSDME expression in cancer cells is a critical determinant of its function and modulates the decision to switch between apoptosis and pyroptosis in cancer cells (66). Although the decrease in expression of N-terminal fragment of GSDME was too small in the present study to definitively conclude that NEAT1/miR-448 directly regulated the cleavage of GSDME, it can still be proposed that the cleavage of GSDME is affected by NEAT1/miR-448 via reduced total expression of GSDME.

The present study has certain shortcomings. For example, more colorectal cancer cell lines should be used to investigate the cell variability and whether NEAT1 expression is high in all tissues should be assessed. Moreover, GSDME is critical for inducing a switch from apoptosis to pyroptosis (6), which can both be triggered by IR (14); therefore, NEAT1 might be involved in this switching process. Thus, further experiments will be required to address these questions.

In summary, the present study demonstrated IR dose-dependently induced pyroptosis and identified the pyroptosis execution protein GSDME as a target of miR-448. lncRNA NEAT1 sponged miR-448 and regulated IR-induced pyroptosis and cell viability in human colorectal cancer cells via regulating the expression, but not activation of GSDME. The findings of the present study elucidated a novel

pyroptosis-related mechanism by which NEAT1 participates in colorectal cancer progression and laid theoretical foundations for further therapeutic development.

Acknowledgements

Not applicable.

Funding

The study was supported by the Chinese National Natural Science Foundation projects (grant nos. 81773038 and 32071290).

Availability of data and materials

The analyzed data generated during the study are available from the corresponding author upon reasonable request.

Authors' contributions

CG, FS and XZ conceived and designed the experiments. FS, JD, JZ and HF performed the experiments and data analysis. CG wrote the manuscript and it was revised for important intellectual content by XZ. CG and FS confirmed the authenticity of all the raw data. All authors read and approved the final manuscript.

Ethics approval and consent to participate

Not applicable.

Patient consent for publication

Not applicable.

Competing interests

The authors declare that they have no competing interests.

References

1. Lu F, Lan Z, Xin Z, He C, Guo Z, Xia X and Hu T: Emerging insights into molecular mechanisms underlying pyroptosis and functions of inflammasomes in diseases. J Cell Physiol 235: 3207-3221, 2020.
2. Wang YY, Liu XL and Zhao R: Induction of pyroptosis and its implications in cancer management. Front Oncol 9: 971, 2019.
3. Shi J, Zhao Y, Wang K, Shi X, Wang Y, Huang H, Zhuang Y, Cai T, Wang F and Shao F: Cleavage of GSDMD by inflammatory caspases determines pyroptotic cell death. Nature 526: 660-665, 2015.
4. Broz P, Pelegrin P and Shao F: The gasdermins, a protein family executing cell death and inflammation. Nat Rev Immunol 20: 143-157, 2020.
5. Ding J, Wang K, Liu W, She Y, Sun Q, Shi J, Sun H, Wang DC and Shao F: Pore-forming activity and structural autoinhibition of the gasdermin family. Nature 535: 111-116, 2016.
6. Wang Y, Gao W, Shi X, Ding J, Liu W, He H, Wang K and Shao F: Chemotherapy drugs induce pyroptosis through caspase-3 cleavage of a gasdermin. Nature 547: 99-103, 2017.
7. An H, Heo JS, Kim P, Lian Z, Lee S, Park J, Hong E, Pang K, Park Y, Ooshima A, *et al*: Tetraarsenic hexoxide enhances generation of mitochondrial ROS to promote pyroptosis by inducing the activation of caspase-3/GSDME in triple-negative breast cancer cells. Cell Death Dis 12: 159, 2021.
8. Zhang CC, Li CG, Wang YF, Xu LH, He XH, Zeng QZ, Zeng CY, Mai FY, Hu B and Ouyang DY: Chemotherapeutic paclitaxel and cisplatin differentially induce pyroptosis in A549 lung cancer cells via caspase-3/GSDME activation. Apoptosis 24: 312-325, 2019.
9. Wang Y, Yin B, Li D, Wang G, Han X and Sun X: GSDME mediates caspase-3-dependent pyroptosis in gastric cancer. Biochem Biophys Res Commun 495: 1418-1425, 2018.
10. Yu J, Li S, Qi J, Chen Z, Wu Y, Guo J, Wang K, Sun X and Zheng J: Cleavage of GSDME by caspase-3 determines lobaplatin-induced pyroptosis in colon cancer cells. Cell Death Dis 10: 193, 2019.
11. Chen MY, Ye XJ, He XH and Ouyang DY: The signaling pathways regulating NLRP3 inflammasome activation. Inflammation 44: 1229-1245, 2021.
12. Ju X, Yang Z, Zhang H and Wang Q: Role of pyroptosis in cancer cells and clinical applications. Biochimie 185: 78-86, 2021.
13. Skandarajah AR, Lynch AC, Mackay JR, Ngan S and Heriot AG: The role of intraoperative radiotherapy in solid tumors. Ann Surg Oncol 16: 735-744, 2009.
14. Batar B, Mutlu T, Bostanci M, Akin M, Tuncdemir M, Bese N and Guven M: DNA repair and apoptosis: Roles in radiotherapy-related acute reactions in breast cancer patients. Cell Mol Biol (Noisy-le-grand) 64: 64-70, 2018.
15. Xiao J, Wang C, Yao JC, Alippe Y, Yang T, Kress D, Sun K, Kostecki KL, Monahan JB, Veis DJ, *et al*: Radiation causes tissue damage by dysregulating inflammasome-gasdermin D signaling in both host and transplanted cells. PLoS Biol 18: e3000807, 2020.
16. Liao H, Wang H, Rong X, Li E, Xu RH and Peng Y: Mesenchymal stem cells attenuate radiation-induced brain injury by inhibiting microglia pyroptosis. Biomed Res Int 2017: 1948985, 2017.
17. Gao J, Peng S, Shan X, Deng G, Shen L, Sun J, Jiang C, Yang X, Chang Z, Sun X, *et al*: Inhibition of AIM2 inflammasome-mediated pyroptosis by Andrographolide contributes to amelioration of radiation-induced lung inflammation and fibrosis. Cell Death Dis 10: 957, 2019.
18. Wu D, Han R, Deng S, Liu T, Zhang T, Xie H and Xu Y: Protective effects of flagellin A N/C against radiation-induced NLR pyrin domain containing 3 inflammasome-dependent pyroptosis in intestinal cells. Int J Radiat Oncol Biol Phys 101: 107-117, 2018.
19. Liu YG, Chen JK, Zhang ZT, Ma XJ, Chen YC, Du XM, Liu H, Zong Y and Lu GC: NLRP3 inflammasome activation mediates radiation-induced pyroptosis in bone marrow-derived macrophages. Cell Death Dis 8: e2579, 2017.
20. Bergmann JH and Spector DL: Long non-coding RNAs: Modulators of nuclear structure and function. Curr Opin Cell Biol 26: 10-18, 2014.
21. Maruyama R and Suzuki H: Long noncoding RNA involvement in cancer. BMB Rep 45: 604-611, 2012.
22. Yang XD, Xu HT, Xu XH, Ru G, Liu W, Zhu JJ, Wu YY, Zhao K, Wu Y, Xing CG, *et al*: Knockdown of long non-coding RNA HOTAIR inhibits proliferation and invasiveness and improves radiosensitivity in colorectal cancer. Oncol Rep 35: 479-487, 2016.
23. Jing L, Yuan W, Ruofan D, Jinjin Y and Haifeng Q: HOTAIR enhanced aggressive biological behaviors and induced radio-resistance via inhibiting p21 in cervical cancer. Tumour Biol 36: 3611-3619, 2015.
24. Zhou JM, Liang R, Zhu SY, Wang H, Zou M, Zou WJ and Nie SL: LncRNA WWC2-AS1 functions AS a novel competing endogenous RNA in the regulation of FGF2 expression by sponging miR-16 in radiation-induced intestinal fibrosis. BMC Cancer 19: 647, 2019.
25. Zou Y, Yao S, Chen X, Liu D, Wang J, Yuan X, Rao J, Xiong H, Yu S, Yuan X, *et al*: LncRNA OIP5-AS1 regulates radioresistance by targeting DYRK1A through miR-369-3p in colorectal cancer cells. Eur J Cell Biol 97: 369-378, 2018.
26. Tan C, Liu W, Zheng ZH and Wan XG: LncRNA HOTTIP inhibits cell pyroptosis by targeting miR-148a-3p/AKT2 axis in ovarian cancer. Cell Biol Int 45: 1487-1497, 2021.
27. Xu Y, Fang H, Xu Q, Xu C, Yang L and Huang C: LncRNA GAS5 inhibits NLRP3 inflammasome activation-mediated pyroptosis in diabetic cardiomyopathy by targeting miR-34b-3p/AHR. Cell Cycle 19: 3054-3065, 2020.
28. She Q, Shi P, Xu SS, Xuan HY, Tao H, Shi KH and Yang Y: DNMT1 methylation of LncRNA GAS5 leads to cardiac fibroblast pyroptosis via affecting NLRP3 axis. Inflammation 43: 1065-1076, 2020.

29. Meng L, Lin H, Zhang J, Lin N, Sun Z, Gao F, Luo H, Ni T, Luo W, Chi J and Guo H: Doxorubicin induces cardiomyocyte pyroptosis via the TINCR-mediated posttranscriptional stabilization of NLR family pyrin domain containing 3. J Mol Cell Cardiol 136: 15-26, 2019.
30. Cui J, Fu HJ, Feng JJ, Zhu J, Tie Y, Xing RY, Wang CF and Zheng XF: The construction of miRNA expression library for human. Prog Biochem Biophy 34: 389-394, 2007.
31. Kong Y, Feng Z, Chen A, Qi Q, Han M, Wang S, Zhang Y, Zhang X, Yang N, Wang J, *et al*: The natural flavonoid galangin elicits apoptosis, pyroptosis, and autophagy in glioblastoma. Front Oncol 9: 942, 2019.
32. Li X, Wang X, Song W, Xu H, Huang R, Wang Y, Zhao W, Xiao Z and Yang X: Oncogenic properties of NEAT1 in prostate cancer cells depend on the CDC5L-AGRN transcriptional regulation circuit. Cancer Res 78: 4138-4149, 2018.
33. Livak KJ and Schmittgen TD: Analysis of relative gene expression data using real-time quantitative PCR and the 2(-Delta Delta C(T)) method. Methods 25: 402-408, 2001.
34. Rogers CJ, Lukaszewicz AI, Yamada-Hanff J, Micewicz ED, Ratikan JA, Starbird MA, Miller TA, Nguyen C, Lee JT, Olafsen T, *et al*: Identification of miRNA signatures associated with radiation-induced late lung injury in mice. PLoS One 15: e0232411, 2020.
35. Tang Z, Li C, Kang B, Gao G, Li C and Zhang Z: GEPIA: A web server for cancer and normal gene expression profiling and interactive analyses. Nucleic Acids Res 45: W98-W102, 2017.
36. Cai J, Yi M, Tan Y, Li X, Li G, Zeng Z, Xiong W and Xiang B: Natural product triptolide induces GSDME-mediated pyroptosis in head and neck cancer through suppressing mitochondrial hexokinase-II. J Exp Clin Cancer Res 40: 190, 2021.
37. Cao X, Wen P, Fu Y, Gao Y, Qi X, Chen B, Tao Y, Wu L, Xu A, Lu H and Zhao G: Radiation induces apoptosis primarily through the intrinsic pathway in mammalian cells. Cell Signal 62: 109337, 2019.
38. Treiber T, Treiber N and Meister G: Regulation of microRNA biogenesis and function. Thromb Haemost 107: 605-610, 2012.
39. Bamodu OA, Huang WC, Lee WH, Wu A, Wang LS, Hsiao M, Yeh CT and Chao TY: Aberrant KDM5B expression promotes aggressive breast cancer through MALAT1 overexpression and downregulation of hsa-miR-448. BMC Cancer 16: 160, 2016.
40. Jiang X, Zhou Y, Sun AJ and Xue JL: NEAT1 contributes to breast cancer progression through modulating miR-448 and ZEB1. J Cell Physiol 233: 8558-8566, 2018.
41. Deng J, Deng H, Liu C, Liang Y and Wang S: Long non-coding RNA OIP5-AS1 functions as an oncogene in lung adenocarcinoma through targeting miR-448/Bcl-2. Biomed Pharmacother 98: 102-110, 2018.
42. Zhao L, Kong H, Sun H, Chen Z, Chen B and Zhou M: LncRNA-PVT1 promotes pancreatic cancer cells proliferation and migration through acting as a molecular sponge to regulate miR-448. J Cell Physiol 233: 4044-4055, 2018.
43. Pei X, Wang X and Li H: LncRNA SNHG1 regulates the differentiation of Treg cells and affects the immune escape of breast cancer via regulating miR-448/IDO. Int J Biol Macromol 118: 24-30, 2018.
44. Ghandhi SA, Smilenov LB, Elliston CD, Chowdhury M and Amundson SA: Radiation dose-rate effects on gene expression for human biodosimetry. BMC Med Genomics 8: 22, 2015.
45. Caudell DL, Michalson KT, Andrews RN, Snow WW, Bourland JD, DeBo RJ, Cline JM, Sempowski GD and Register TC: Transcriptional profiling of non-human primate lymphoid organ responses to total-body irradiation. Radiat Res 192: 40-52, 2019.
46. Lu X, Ma O, Nguyen TA, Jones SN, Oren M and Donehower LA: The Wip1 Phosphatase acts as a gatekeeper in the p53-Mdm2 autoregulatory loop. Cancer Cell 12: 342-354, 2007.
47. Ge C, Su F, Fu H, Wang Y, Tian B, Liu B, Zhu J, Ding Y and Zheng X: RNA profiling reveals a common mechanism of histone gene downregulation and complementary effects for radioprotectants in response to ionizing radiation. Dose Response: Oct 16, 2020 (Epub ahead of print).
48. Wang Y, Chen X, Tsai S, Thomas A, Shizuru JA and Cao TM: Fine mapping of the Bmgr5 quantitative trait locus for allogeneic bone marrow engraftment in mice. Immunogenetics 65: 585-596, 2013.
49. Chao L, Li Z, Zhou J, Chen W, Li Y, Lv W, Guo A, Qu Q and Guo S: Shen-Ling-Bai-Zhu-San improves dextran sodium sulfate-induced colitis by inhibiting caspase-1/caspase-11-mediated pyroptosis. Front Pharmacol 11: 814, 2020.
50. Jie F, Xiao S, Qiao Y, You Y, Feng Y, Long Y, Li S, Wu Y, Li Y and Du Q: Kuijieling decoction suppresses NLRP3-Mediated pyroptosis to alleviate inflammation and experimental colitis in vivo and in vitro. J Ethnopharmacol 264: 113243, 2021.
51. Deng Z, Ni J, Wu X, Wei H and Peng J: GPA peptide inhibits NLRP3 inflammasome activation to ameliorate colitis through AMPK pathway. Aging (Albany NY) 12: 18522-18544, 2020.
52. Wu T, Liu W, Fan T, Zhong H, Zhou H, Guo W and Zhu X: 5-Androstenediol prevents radiation injury in mice by promoting NF-κB signaling and inhibiting AIM2 inflammasome activation. Biomed Pharmacother 121: 109597, 2020.
53. Wu LS, Liu Y, Wang XW, Xu B, Lin YL, Song Y, Dong Y, Liu JL, Wang XJ, Liu S, *et al*: LPS enhances the chemosensitivity of oxaliplatin in HT29 cells via GSDMD-mediated pyroptosis. Cancer Manag Res 12: 10397-10409, 2020.
54. Wang H, Lu B and Chen J: Knockdown of lncRNA SNHG1 attenuated $A\beta_{25-35}$-inudced neuronal injury via regulating KREMEN1 by acting as a ceRNA of miR-137 in neuronal cells. Biochem Biophys Res Commun 518: 438-444, 2019.
55. Liu X, Song W, Zhang X, Long F, Yin J, He X and Lv L: Downregulating LncRNA XIST attenuated contrast-induced nephropathy injury via regulating miR-133a-3p/NLRP3 axis. J Thromb Thrombolysis: Jan 2, 2021 (Epub ahead of print). doi: 10.1007/s11239-020-02369-0.
56. Meng J, Ding T, Chen Y, Long T, Xu Q, Lian W and Liu W: LncRNA-Meg3 promotes Nlrp3-mediated microglial inflammation by targeting miR-7a-5p. Int Immunopharmacol 90: 107141, 2021.
57. Zhong F, Zhang W, Cao Y, Wen Q, Cao Y, Lou B, Li J, Shi W, Liu Y, Luo R and Chen C: LncRNA NEAT1 promotes colorectal cancer cell proliferation and migration via regulating glial cell-derived neurotrophic factor by sponging miR-196a-5p. Acta Biochim Biophys Sin (Shanghai) 50: 1190-1199, 2018.
58. Liu H, Li A, Sun Z, Zhang J and Xu H: Long non-coding RNA NEAT1 promotes colorectal cancer progression by regulating miR-205-5p/VEGFA axis. Hum Cell 33: 386-396, 2020.
59. Liu F, Ai FY, Zhang DC, Tian L, Yang ZY and Liu SJ: LncRNA NEAT1 knockdown attenuates autophagy to elevate 5-FU sensitivity in colorectal cancer via targeting miR-34a. Cancer Med 9: 1079-1091, 2020.
60. Wang X, Jiang G, Ren W, Wang B, Yang C and Li M: LncRNA NEAT1 regulates 5-Fu sensitivity, apoptosis and invasion in colorectal cancer through the MiR-150-5p/CPSF4 axis. Onco Targets Ther 13: 6373-6383, 2020.
61. Han D, Wang J and Cheng G: LncRNA NEAT1 enhances the radio-resistance of cervical cancer via miR-193b-3p/CCND1 axis. Oncotarget 9: 2395-2409, 2017.
62. Lu Y, Li T, Wei G, Liu L, Chen Q, Xu L, Zhang K, Zeng D and Liao R: The long non-coding RNA NEAT1 regulates epithelial to mesenchymal transition and radioresistance in through miR-204/ZEB1 axis in nasopharyngeal carcinoma. Tumour Biol 37: 11733-11741, 2016.
63. Blume CJ, Hotz-Wagenblatt A, Hüllein J, Sellner L, Jethwa A, Stolz T, Slabicki M, Lee K, Sharathchandra A, Benner A, *et al*: p53-dependent non-coding RNA networks in chronic lymphocytic leukemia. Leukemia 29: 2015-2023, 2015.
64. Shamloo B and Usluer S: p21 in cancer research. Cancers (Basel) 11: 1178, 2019.
65. Guo L, Huang S and Wang X: PUMA mediates the anti-cancer effect of osimertinib in colon cancer cells. Onco Targets Ther 10: 5281-5288, 2017.
66. Jiang M, Qi L, Li L and Li Y: The caspase-3/GSDME signal pathway as a switch between apoptosis and pyroptosis in cancer. Cell Death Discov 6: 112, 2020.